# Microwave interferometer for steady-state plasmas

Earl E. Scime, Robert F. Boivin, John L. Kline, and Matthew M. Balkey
*Department of Physics, West Virginia University, Morgantown, West Virginia 26506-6315*

(Received 2 October 2000; accepted for publication 27 November 2000)

Standard single frequency, ''fringe-counting,'' microwave interferometers are of limited use for steady-state plasma experiments. We have constructed a swept frequency microwave interferometer, similar to a classic zebra-stripe interferometer, optimized for electron density measurements in steady-state plasma experiments. The key element in the system is a frequency doubled YIG oscillator capable of sweeping from 20 to 40 GHz. As the source frequency is swept, the sum of the reference and plasma leg signals exhibits a series of beats. Both the frequency shift and phase shift of the beat pattern due to the addition of plasma in one leg of the interferometer is used to determine the line-integrated electron density. © *2001 American Institute of Physics.*
[DOI: 10.1063/1.1347971]

## I. INTRODUCTION

We have developed a relatively simple microwave interferometer that can be used to directly measure the electron density in steady-state plasma experiments. The technique is based on the ''zebra-stripe'' systems developed for pulsed plasma experiments in the 1950's and 1960's.[1,2] Essentially, the zebra-stripe technique is a graphical means of counting fringes, i.e., phase shifts of $2\pi$, that arise as the plasma density increases from zero in a pulsed experiment. At the heart of a standard zebra-stripe system is a swept frequency microwave source that is rapidly ramped through a narrow frequency band. The ramp period is short compared to the time span of the plasma discharge and the combination of a long reference leg and the frequency sweep generates a series of interference fringes or zebra stripes that shift in overall phase during the plasma discharge. The zebra stripes are due to the frequency dependent differences in time-of-flight for the microwaves between the reference and the plasma legs of the interferometer as the source frequency is varied.

The fundamental operational difference between the system described here and the classic zebra-stripe system is that, in a steady-state system, there is no overall shift of the fringe pattern as the plasma forms and the density increases. Instead, the overall phase shift and beat frequency of the net signal is measured with and without plasma in the plasma leg of the interferometer. The line averaged electron density can then be determined from a nonlinear fit to the frequency dependent phase shift pattern. In addition, the long waveguide sections used in zebra-stripe systems to generate a sufficient number of fringes from a small frequency variation are not required. In fact, in this approach, the relative effect of the plasma on the phase shift pattern is enhanced by making the lengths of the plasma and reference legs nearly equal. Another key feature of this diagnostic is that losses due to refraction and reflection are only significant if they reduce the transmitted signal to undetectable levels.

In the following sections, we describe the operational principles behind the design of the diagnostic, the experimental apparatus used, and typical experimental results.

## II. OPERATIONAL PRINCIPLES

Given the geometry shown in Fig. 1, the net time varying signal due to the superposition each of the sinusoidal signals from each leg of the interferometer is given by

$$M(t)=2A\sin[\omega_\mu t+\tfrac{1}{2}(\phi_1+\phi_p+\phi_2)]\cos[\omega_\mu t+\tfrac{1}{2}(\phi_1-\phi_p-\phi_2)]+2(B-A)\sin[\omega_\mu t+\phi_p+\phi_2], \quad (1)$$

where $A$ and $B$ are the amplitudes of the plasma and reference leg signals respectively, $\omega_\mu$ is the microwave source frequency, $\phi_1$ is the phase shift due to dispersion in waveguide in the reference leg, $\phi_2$ is the phase shift due to dispersion in waveguide in the plasma leg, and $\phi_p$ is the phase shift due to dispersion in the plasma. Since the crystal detector measures time averaged power, the detector signal can be written as

$$S(t)\propto 2A^2\cos^2[\tfrac{1}{2}(\phi_1-\phi_p-\phi_2)], \quad (2)$$

where the rate of change in the phase shift due to changing the microwave frequency is assumed to be slow compared to the microwave frequency, i.e., $(1/\omega)(d\omega/dt)\ll\omega$, and the signal amplitudes from each leg are assumed to be equal, $B=A$. Unequal signal strengths simply add a constant term to Eq. (2). Equation (2) suggests that if it is possible to design a system such that the net phase difference as the source frequency is varied is a linear function of time, the detector signal can be described solely in terms of a constant ''beat'' frequency, i.e., $S(t)\propto\cos^2(\omega_{\text{beat}}t)$.

The same mathematical result is achieved if the system is treated in terms of time-of-flight for the microwaves traveling through each leg. Due to the less than unity index of refraction of the plasma, the introduction of plasma shortens the time-of-flight for the microwaves in the plasma leg. Since the index of refraction of the plasma depends on the plasma density, the difference in the time-of-flight will depend on the plasma density. Thus, the time-of-flight calculation yields the same result as the superposition approach of Eq. (2).

The phase shifts in Eq. (2) are given by

 

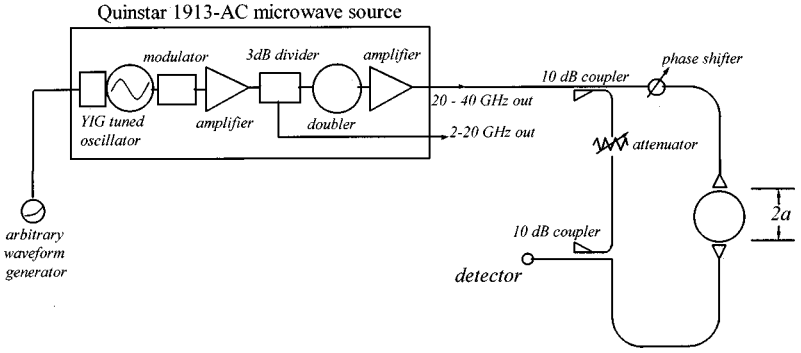


FIG. 1. Schematic of the microwave system including the source and waveguide structures.

$$\phi_1(\omega)=\int_{\text{reference leg}} k_g dl,$$

$$\phi_2(\omega)=\int_{\text{plasma leg}} k_g dl, \tag{3}$$

$$\phi_p(\omega)=\int_{\text{plasma}} k_p dl,$$

where $k_g=(1/c)\sqrt{\omega^2-\omega_c^2}$ is the wave number in the waveguide, $\omega_c$ is the cutoff frequency in the waveguide, $k_p=(1/c)\sqrt{\omega^2-\omega_p^2}$ is the wave number in the plasma, $\omega_p^2=(4\pi n_e e^2/m_e)$ is the plasma frequency, $\omega$ is the source frequency, $n_e$ is the plasma density, $e$ is the electron charge, and $m_e$ is the electron mass. Assuming the wave number in the waveguide is constant for a fixed frequency, the time rate of change of the total phase difference between the reference and plasma leg signals is

$$\frac{\partial \Delta\phi}{\partial t}=\frac{\partial \omega}{\partial t}\left(\Delta L\frac{\partial k_g}{\partial \omega}+\int_{-a}^{a}\frac{\partial k_p}{\partial \omega}dl\right), \tag{4}$$

where the time dependence of the source frequency has been extracted from the line integrals, $a$ is the plasma radius, and $\Delta L$ is the net difference in waveguide length between the plasma and reference legs.

A key functional aspect of this diagnostic is the change in the beat frequency, $\omega_B=\partial\Delta\phi/\partial t$, due to the plasma. The time dependence of the source frequency sweep can be determined by requiring that the beat frequency in the absence of plasma, $\omega_{B0}=\partial\Delta\phi/\partial t$, be a constant

$$\omega_{B_0}=\frac{\partial \omega}{\partial t}\left(\Delta L\frac{\partial k_g}{\partial \omega}+\frac{2a}{c}\right)=\text{constant}. \tag{5}$$

A typical nonlinear source frequency sweep satisfying Eq. (5) is shown in Fig. 2. The hardware needed to generate such a frequency sweep is discussed in Sec. III. An important feature of Eq. (5) is that the beat frequency consists of two ''parts:'' the waveguide effect and the plasma path effect. To maximize the effect of the plasma on the beat frequency, it is desirable for the length of the plasma to be comparable to the difference in waveguide lengths of the two legs of the system. Thus, the ideal design of this system differs significantly from a classic zebra-stripe interferometer where the difference in waveguide lengths is maximized in order to generate as many fringes as possible per change in source frequency.

Given a constant beat frequency in the absence of plasma, the logical experimental procedure is to add plasma to the system, measure the change in the beat frequency, and extract the line-integrated density according to Eq. (4). In fact, for specific choices of density profiles, i.e., parabolic, cubic, etc., it is possible to derive either exact or convergent series expressions that can be used to calculate the peak density along the microwave path through the plasma. For example, the peak plasma density for a parabolic density profile, $n_e(r)=n_0[1-(r/a)^2]$, is related to the shift in beat frequency, $\Delta\omega=\omega_B-\omega_{B0}$, by

$$\frac{1}{3}\left(\frac{\omega_{\text{po}}}{\omega}\right)^2+\frac{1}{5}\left(\frac{\omega_{\text{po}}}{\omega}\right)^4+\cdots\frac{1}{n}\left(\frac{\omega_{\text{po}}}{\omega}\right)^{n-1}$$

$$=\left(\frac{c}{2a}\right)\left(\frac{1}{\partial\omega/\partial t}\right)\Delta\omega, \tag{6}$$

where $\omega>\omega_p$ everywhere in the plasma and $\omega_{\text{po}}$ is the peak plasma frequency, i.e., the peak plasma density. Note that Eq. (6) does not require the assumption that $\omega\gg\omega_p$ in the plasma. However, because the change in the beat frequency only becomes significant for microwave frequencies near the plasma frequency, we have found that operating near the peak plasma frequency and fitting the measured beat signal to Eq. (2) yields the most reliable measurement of the plasma density. By using both the phase and frequency shift information in the measured signal and assuming a particular density profile, the peak line-of-sight density can be determined for different choices of the density profile. Because the sys-

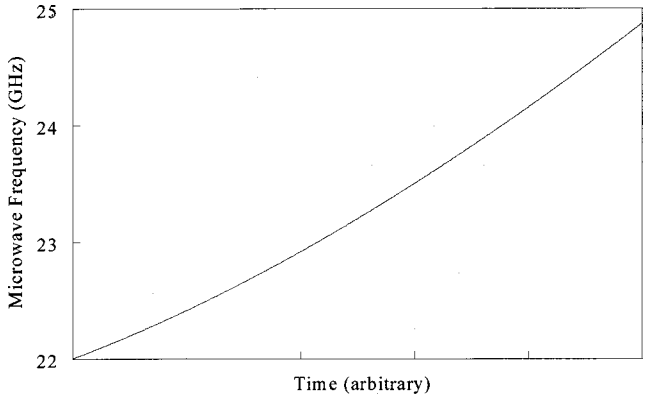


FIG. 2. Typical nonlinear frequency sweep that satisfies the constant beat frequency requirement described by Eq. (5). In this case, a waveguide cutoff frequency of 20.37 GHz was used.

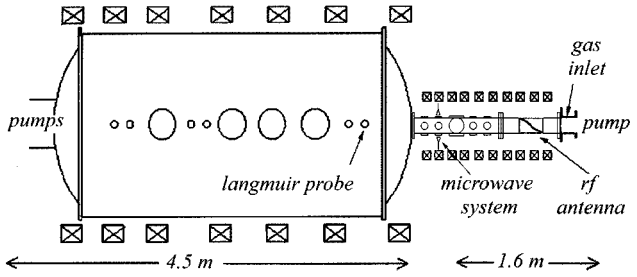


FIG. 3. Schematic of the combined helicon source and space plasma simulation chamber apparatus. The microwave horns are inside the vacuum system at the port indicated. The Langmuir probe measures the downstream plasma density in the space simulation chamber and the laser induced fluorescence system measures the qualitative density profile at the location of the large port adjacent to the microwave system.

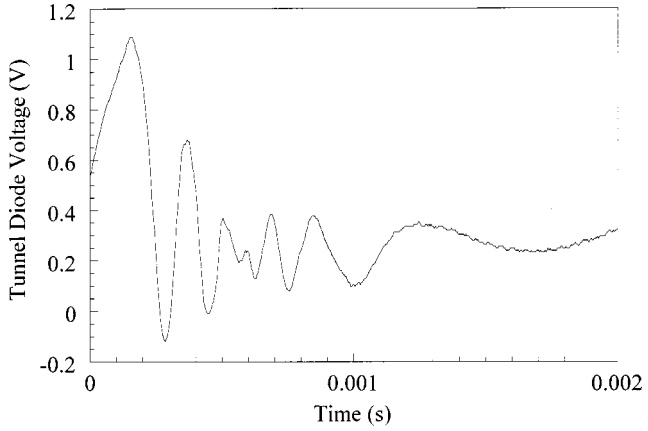


FIG. 4. Tunnel diode signal during pulsed plasma operation showing seven $2\pi$ phase shifts for 33.6 GHz microwaves.

tem operates just above the peak plasma frequency in the plasma, it is not possible to avoid choosing a density profile as is typically done with microwave interferometers that operate well above the peak plasma frequency. Those diagnostics yield a line-of-sight averaged electron density based solely on the measured phase shift.

We will show that the results of the nonlinear fits to Eq. (2) are consistent with Langmuir probe measurements of the on-axis density, standard fringe counting in pulsed discharges, and qualitative profile measurements of the ion density. For use in nonlinear fitting algorithms, the detailed version of Eq. (2), in terms of the source frequency, is

$$S(\omega)\propto 2A^2\cos^2\left\{\left[\Delta L\sqrt{\omega^2-\omega_c^2}+\int_{-a}^{a}\sqrt{\omega^2-\omega_p^2(l)}dl\right]\Big/\,2c\right\}. \tag{7}$$

Here again, the relative change in the frequency of the beat pattern with the addition of plasma is maximized if $\Delta L$ is kept to a minimum. The disadvantage of a small waveguide length difference, $\Delta L$, is that the source frequency must be swept over a larger frequency range in order to generate a sufficient number of fringes.

## III. EXPERIMENTAL APPARATUS

As shown in Fig. 1, the microwave source is based on a frequency-doubled, tuned YIG oscillator built by Quinstar Technology Inc. The source generates microwaves in either of two frequency bands: 2–20 and 20–40 GHz. Each band has a nominal power of 20 mW. The source can be modulated through an in-line pin modulator and the operating frequency in each band is selected via a 0–10 V control signal. Frequency sweeps, such as the one shown in Fig. 2, are numerically computed and loaded into a HP33120A arbitrary wave form generator via a general purpose interface bus. The detector is a Herotek 2–40 GHz tunnel diode. The signal from the tunnel diode is recorded on a digital oscilloscope during pulsed-mode operation of the source and with a VXI-based digitizer during steady-state operation.

The configuration of plasma experiment is shown in Fig. 3. WR-28 waveguide is used throughout the system. Microwave power is coupled into the internal horns through Kapton™ microwave windows (Microtech) mounted in standard 2 3/4 in. Conflat™ vacuum flanges. The horns are designed to operate in the far field, Fraunhofer, diffraction regime as the number of exposed Fresnel zones, $n$,[3]

$$n=(X^2/4\lambda)(1/L+1/R) \tag{8}$$

is less than one. $X$ is the length of the horn aperture along the magnetic field (to ensure launching the correction polarization, the short axis of the horn ($X=1.6$ cm) must be aligned with the magnetic field),[1] $\lambda$ is the microwave wavelength, $L$ is the length of the horn ($L=4.5$ cm), and $R$ is the distance from the end of the horn to the center of the plasma column ($R\sim 10.8$ cm). For our system parameters and $\lambda$ calculated for 30 GHz microwaves, $n\sim 0.2$ is obtained. The width of the central maximum of the diffraction pattern ($\sim 2\lambda R/X$) is on the order of 12 cm. A wide central maximum has the advantage of illuminating the plasma column with a microwave field much wider than the typical bright center of a helicon discharge.[4,5] However, diffracted rays can still reach the receiving horn on the far side of the discharge when the central density is high enough to cutoff the microwave signal in the middle of the discharge ($\omega<\omega_{po}$). Thus, attempts to measure the peak density by simply looking for the cutoff frequency have been equivocal.

Our plasma discharge operates in either a steady state or a pulsed mode. When operating in a pulsed mode, standard fringe ($2\pi$ phase shift) counting for a fixed microwave frequency can be used to determine the change in line-averaged density during the startup of the plasma. A typical pulsed mode operation 33.6 GHz microwave signal is shown in Fig. 4. Depending on the density profile, linear or parabolic, each of the seven fringes corresponds to change in the peak density of $3.4\times 10^{12}\,\mathrm{cm}^{-3}$ or $2.3\times 10^{12}\,\mathrm{cm}^{-3}$, respectively. A comparison of the number of microwave fringes and the density as measured with a radio frequency (rf)-compensated Langmuir probe[4,6] for a scan of source magnetic field strength is shown in Fig. 5. Note that the Langmuir probe is in the expansion chamber downstream from the source. Depending on the neutral pressure and the operational mode of the source (capacitive, inductive, or helicon), the plasma

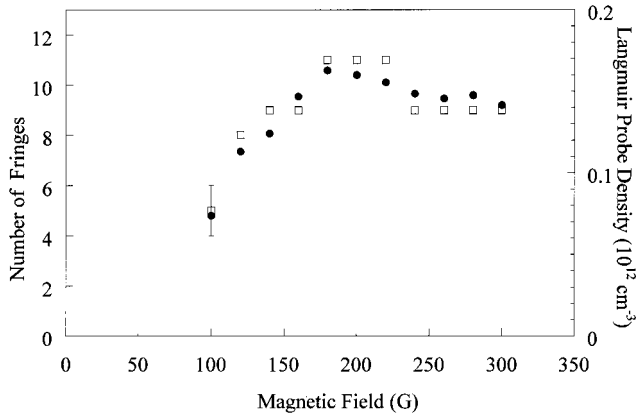


FIG. 5. Comparison of the number of microwave interference fringes (open squares) obtained at startup for 33.6 GHz microwaves and the downstream density measured with a Langmuir probe (filled circles) during pulsed operation of the plasma source. A typical error bar representative of the statistical error in the number of fringes is shown for the 100 G field data point. The statistical errors in the Langmuir probe data are smaller than the size of the data points used. Both diagnostics show the same relative changes in electron density as a function of source magnetic field strength.

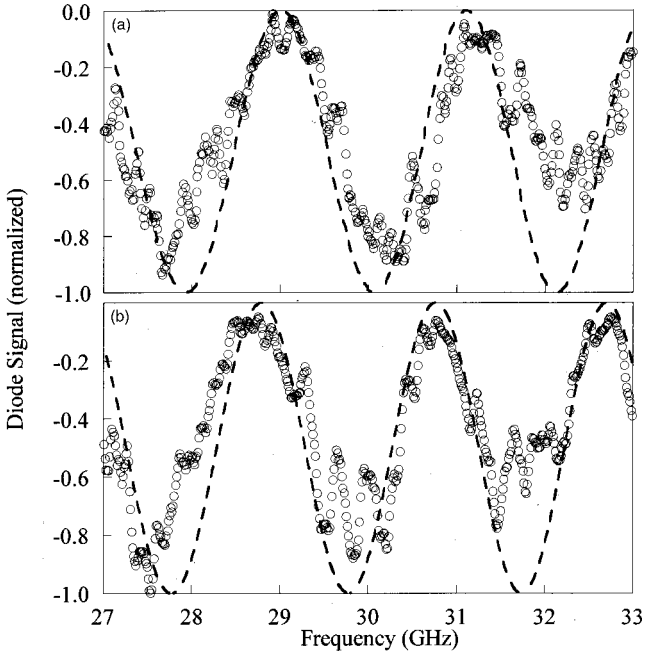


FIG. 6. (a) Beat pattern obtained without plasma. (b) Beat pattern obtained with plasma. Dotted lines are nonlinear fits of Eq. (7) to the measurements.

density in the source is 10–100 times larger than the plasma density in the expansion chamber. Based the data in Fig. 5, we have concluded that the microwave measurements in the source are consistent with the downstream Langmuir probe measurements for pulsed mode operation.

## IV. EXPERIMENTAL RESULTS

During steady-state operation of the source, the microwave frequency can be swept in a fashion similar to Fig. 2 if a constant beat frequency is desired. Since we fit the entire measured beat pattern as a function of source frequency to equation (7), a simple linear frequency ramp is sufficient. For reference, the same frequency sweep is performed with and without plasma. Typical measurements without and with plasma are shown in Figs. 6(a) and 6(b) respectfully. The beat pattern for the case without plasma is well fit by Eq. (7) using the measured plasma horn-to-horn spacing of 21.54 cm and the measured difference in waveguide length of 5.1 cm. With the introduction of plasma into the plasma leg of the system, there is a clear increase in the frequency of the beat pattern. A nonlinear fit of Eq. (7) to the measurements yields a peak density of $3.7\times10^{12}\,\mathrm{cm}^{-3}$ for a sharply peaked density profile, $n_e(r)\sim n_0[1-(r/a)^{0.3}]$. Fixed microwave frequency measurements for pulsed source operation at the same plasma parameters yielded 1.5–2 fringes at 33.6 GHz, consistent with the steady-state phase shift and frequency change peak density result of $3.7\times10^{12}\,\mathrm{cm}^{-3}$.

To determine if the density profile is as steep as suggested by the fit to the swept frequency microwave measurements, we measured the emission intensity profile of fluorescing argon ions with a two-dimensional scanning laser induced fluorescence (LIF) diagnostic. The absorption and emission frequencies of an atom or ion moving relative to a radiation source are Doppler shifted by its velocity. In a typical LIF measurement, the frequency of a very narrow bandwidth laser is swept across a collection of ions or atoms that have a thermally broadened velocity distribution. Ions at the appropriate velocity relative to the beam absorb a photon and the fluorescent emission that results after the excited electrons decay to a lower energy state is measured.[7] The shift in the center frequency and the width of the absorption spectrum feature for the entire ensemble of atoms or ions is then used to determine the temperature and flow velocity of the particle distribution.[8] The signal intensity is directly proportional to the density of ions in the LIF pumped metastable state. A radial profile of LIF intensity for the same source parameters is shown in Fig. 7(a). Assuming the electron temperature is approximately constant across the 8 cm of the discharge shown in Fig. 7(a), the density of ions in the metastable state is directly proportional to the total ion density. Thus, the LIF intensity profile is a direct measure of the plasma density profile in the source. The LIF system has a 0.5 cm spatial resolution due to the size of the region where the laser beam and the field-of-view of the collection optics overlap. The LIF data clearly indicate a hollow density profile. If the swept frequency microwave data is fit with the model density profile shown in Fig. 7(a) as a dotted line, the peak density that yields the best fit is $3.5\times10^{12}\,\mathrm{cm}^{-3}$ [shown as a solid line in Fig. 7(b)]. The sensitivity of the fitting process to the peak density is demonstrated by the dotted line in Fig. 7(b) that corresponds to a peak density of $4.0\times10^{12}\,\mathrm{cm}^{-3}$. With either the sharply peaked or hollow density profile, the only significant contribution to the frequency and phase shifts of the microwave signal is made by the localized region of peak density. Since these regions are similar in size in both cases, the best-fit peak densities are similar in magnitude.

To compare the downstream plasma densities measured with the Langmuir probe to the swept frequency microwave measurements, a rf power scan experiment was conducted. The results, shown in Fig. 8, indicate that the relative changes in the plasma density obtained from fits to the mi-

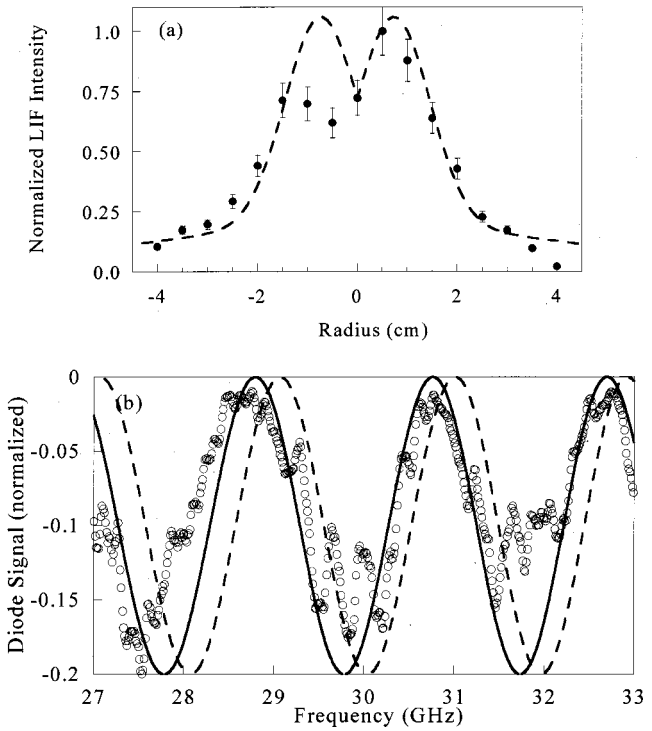


FIG. 7. (a) Normalized LIF intensity profile over the inner 8 cm of the discharge (solid circles) and a model fit to the density profile based on the equation $I=0.245\ [1-(|r|/a)^{0.9}]+0.84\exp[-(|r|-.75)^2/(0.1a)^2]$ (solid line). The error bars indicate the statistical error in each data point. (b) Beat pattern obtained with plasma (solid circles); nonlinear fit of Eq. (7) using the model hollow density profile and a peak density of $3.5\times10^{12}\,\mathrm{cm}^{-3}$ (solid line); nonlinear fit of Eq. (7) using the model hollow density profile and a peak density of $4.0\times10^{12}\,\mathrm{cm}^{-3}$ (dotted line).

crowave data are also consistent with the downstream Langmuir probe measurements.

## V. DISCUSSION

We have demonstrated that a swept frequency microwave interferometer can provide measurements of the line-integrated electron density in a steady-state helicon plasma source. Using model density profiles parametrized in terms of a peak density, measurements of the peak plasma density can be obtained. The experimental results are consistent with

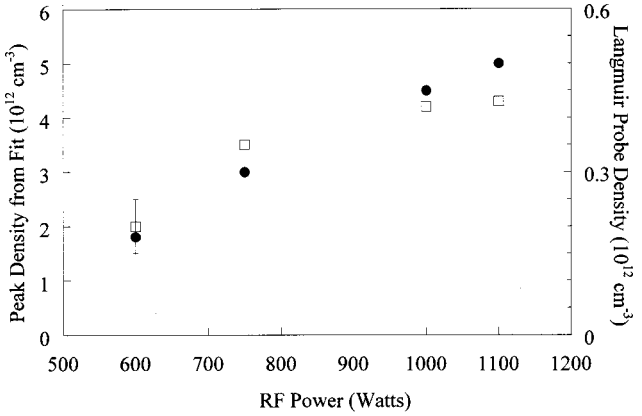


FIG. 8. Comparison of the peak density obtained from the swept frequency microwave system (open squares) and the downstream density measured with a Langmuir probe (filled circles) as a function of source rf power. A typical error bar representative of the uncertainty in the numerical fit is shown for the data point at 600 W. The statistical errors in the Langmuir probe data are smaller than the size of the data points used.

downstream Langmuir probe measurements; pulsed source, single microwave frequency fringe counting; and LIF emission profiles.

## ACKNOWLEDGMENTS

The authors thank Fred Skiff of the University of Iowa for suggesting the central idea of this diagnostic to us during his visit to our laboratory. This work was supported by the National Science Foundation and the U.S. Department of Energy.

[1] M. A. Heald and C. B. Warton, *Plasma Diagnostics with Microwaves* (Wiley, New York, 1965).
[2] I. H. Hutchinson, *Principles of Plasma Diagnostics* (Cambridge University Press, Cambridge, 1987).
[3] R. F. Boivin, WVU Plasma Physics Group Internal Report PLP-043 (1999).
[4] P. A. Keiter, E. E. Scime, and M. M. Balkey, Phys. Plasmas **4**, 2741 (1997).
[5] R. W. Boswell, Phys. Lett. A **33**, 457 (1970).
[6] I. D. Sudit and F. Chen, Plasma Sources Sci. Technol. **3**, 162 (1994).
[7] D. H. Hill, S. Fornaca, and M. G. Wickham, Rev. Sci. Instrum. **54**, 309 (1983).
[8] E. E. Scime, P. A. Keiter, M. W. Zintl, M. M. Balkey, J. L. Kline, and M. E. Koepke, Plasma Sources Sci. Technol. **7**, 186 (1998).